

Article

Correlating Remote Sensing Data with the Abundance of Pupae of the Dengue Virus Mosquito Vector, *Aedes aegypti*, in Central Mexico

Max J. Moreno-Madriñán ^{1,*}, William L. Crosson ², Lars Eisen ³, Sue M. Estes ⁴, Maurice G. Estes Jr. ⁴, Mary Hayden ⁵, Sarah N. Hemmings ^{2,6}, Dan E. Irwin ⁷, Saul Lozano-Fuentes ³, Andrew J. Monaghan ⁵, Dale Quattrochi ⁷, Carlos M. Welsh-Rodriguez ⁸ and Emily Zielinski-Gutierrez ⁹

¹ Department of Environmental Health, Fairbanks School of Public Health, Indiana University, IUPUI, Indianapolis, IN 46202, USA

² Science and Technology Institute, Universities Space Research Association (USRA), Huntsville, AL 35805, USA; E-Mails: bill.crosson@nasa.gov (W.L.C.); sarah.n.hemmings@nasa.gov (S.N.H.)

³ Department of Microbiology, Immunology and Pathology, Colorado State University, Fort Collins, CO 80523, USA; E-Mails: lars.eisen@colostate.edu (L.E.); saul.lozano-fuentes@colostate.edu (S.L.-F.)

⁴ Earth and System Science Center, University of Alabama in Huntsville, Huntsville, AL 35805, USA; E-Mails: sue.m.estes@nasa.gov (S.M.E.); maury.estes@nsstc.uah.edu (M.G.E.)

⁵ Research Applications Laboratory, National Center for Atmospheric Research, Boulder, CO 80307, USA; E-Mails: monaghan@ucar.edu (M.H.); mhayden@ucar.edu (A.J.M.)

⁶ Earth Science Division, Applied Sciences Program, NASA Headquarters, Washington, DC 20024-3210, USA

⁷ Earth Science, NASA Marshall Space Flight Center, Huntsville, AL 35811, USA; E-Mails: daniel.irwin@nasa.gov (D.E.I.); dale.quattrochi@nasa.gov (D.Q.)

⁸ Earth Sciences Center, Veracruz University, 91090 Xalapa, Mexico; E-Mail: cwelsh@uv.mx

⁹ Division of Vector-Borne Diseases, National Center for Emerging and Zoonotic Infectious Diseases, Centers for Disease Control and Prevention, Fort Collins, CO 80521, USA; E-Mail: Ebz0@cdc.gov

* Author to whom correspondence should be addressed; E-Mail: mmorenom@iu.edu; Tel.: +1-317-274-3170; Fax: +1-317-274-3443.

Received: 24 March 2014; in revised form: 23 April 2014 / Accepted: 29 April 2014 /

Published: 20 May 2014

Abstract: Using a geographic transect in Central Mexico, with an elevation/climate gradient, but uniformity in socio-economic conditions among study sites, this study evaluates the applicability of three widely-used remote sensing (RS) products to link weather conditions with the local abundance of the dengue virus mosquito vector, *Aedes aegypti* (*Ae. aegypti*). Field-derived entomological measures included estimates for the percentage of premises with the presence of *Ae. aegypti* pupae and the abundance of *Ae. aegypti* pupae per premises. Data on mosquito abundance from field surveys were matched with RS data and analyzed for correlation. Daily daytime and nighttime land surface temperature (LST) values were obtained from Moderate Resolution Imaging Spectroradiometer (MODIS)/Aqua cloud-free images within the four weeks preceding the field survey. Tropical Rainfall Measuring Mission (TRMM)-estimated rainfall accumulation was calculated for the four weeks preceding the field survey. Elevation was estimated through a digital elevation model (DEM). Strong correlations were found between mosquito abundance and RS-derived night LST, elevation and rainfall along the elevation/climate gradient. These findings show that RS data can be used to predict *Ae. aegypti* abundance, but further studies are needed to define the climatic and socio-economic conditions under which the correlations observed herein can be assumed to apply.

Keywords: MODIS; TRMM; DEM; Aqua; remote sensing; elevation; mosquito; rainfall; temperature

1. Introduction

Environmental changes potentially impacting the geographical ranges or local abundance of arthropod vectors transmitting infectious disease agents are among the important concerns linked to climate [1–6]. Associations reported in the literature show that climate-related variables can be used to predict local abundance and the potential for the expansion of arthropod vectors, such as mosquitoes or ticks [7–10]. Since field surveys are both costly and time consuming, remote sensing (RS) technology is increasingly used to estimate habitat suitability for a variety of vector species [11–14]. Temperature and rainfall are the weather parameters of special interest, because they impact both the distribution of suitable vector habitat and the potential for local vector proliferation. Although terrain elevation is strongly associated with temperature, urban heat islands might cause slight differences in the associations between vector abundance and climate parameters in studies conducted within urban environments. Thus, elevation is included among the variables of interest for this study. *Aedes aegypti* (*Ae. aegypti*), the primary mosquito vector of dengue and yellow fever viruses and an important vector of chikungunya virus to humans in urban settings, is most abundant in urban environments [15].

Dengue is one of the most important mosquito-borne viral diseases in the subtropics and tropics, with one estimate of the global infection burden reaching approximately 390 million virus infections and nearly 100 million cases with disease manifestations per year, over three times that estimated by the World Health Organization [16]. Although the presence and abundance of the mosquito vector is strongly influenced by the human peridomestic environment (e.g., access to water-holding containers

serving as larval development sites and the potential for intrusion into homes to engage in indoor biting), these are also affected by meteorological variables, such as temperature, rainfall, humidity and solar radiation. Several studies have addressed the relationship between weather or climate variability and the incidence of dengue disease cases [17–28]. Such relationships, however, may be influenced by additional factors, such as the exposure of humans to mosquitos and the intensity of virus transmission [29].

The strength of the association between RS-based climate parameters and vector abundance may be limited by the spatial resolution of the satellite products that are freely available and more commonly used [7]. Environmental and socio-economic conditions can change drastically over distances of 10–100 m of meters; therefore, spatial models designed to estimate vector presence and abundance developed at the regional or state level cannot reliably be down-scaled for locally-relevant risk predictions. To develop models to predict vector presence and abundance at the local (community or neighborhood) scale using RS-based environmental inputs requires consistent monitoring of recent local environmental conditions with RS imagery that can distinguish the differences between adjacent communities or neighborhoods. The present study tests if three widely used RS-based environmental products are able to distinguish those differences at the local level, despite having spatial resolutions equal or larger than 90 m. Our motivation is to evaluate the potential for using RS-based environmental products that are freely-available to decision-makers in developing countries, to monitor the presence and abundance of *Ae. aegypti* at the local scale. For a geographic transect of approximately 330 km by road, corresponding to an area of approximately 245 km (west-east) by 98 km (north-south) in central Mexico, we describe the associations between the presence and abundance of the pupal life stage of *Ae. aegypti* and environmental conditions estimated from RS products, including land surface temperature (LST), rainfall, land surface properties and elevation.

2. Methodology

2.1. Study Site

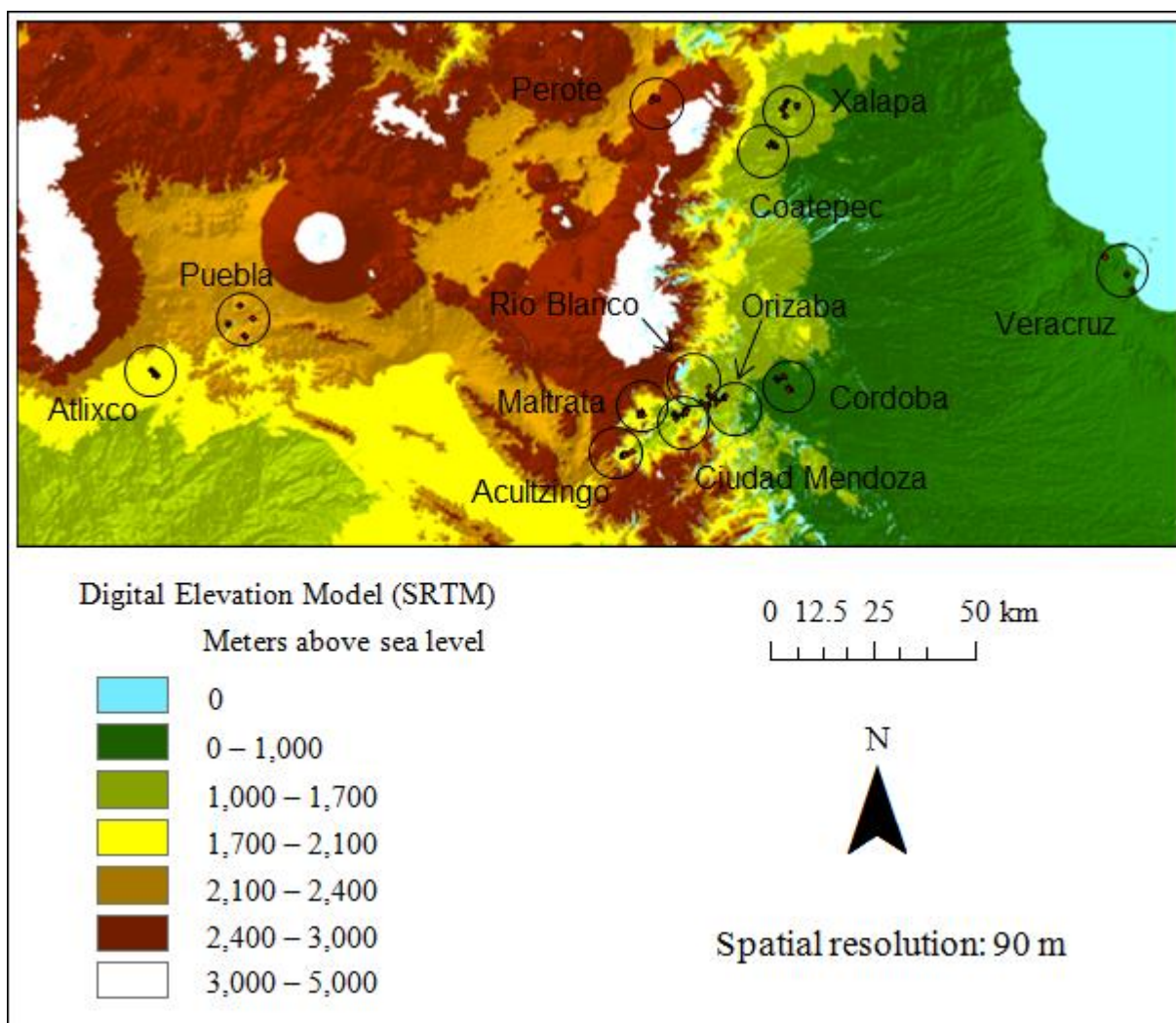
This study used sites from a previously published study [30] on the occurrence of *Ae. aegypti* along the elevation gradient between Veracruz at sea level and Puebla at more than 2000 m in Central Mexico (Figure 1). Sites were composed of groups of homes with low to middle income and small to medium-sized yards, distributed among 12 communities along the elevation gradient described.

2.2. Field Survey Mosquito Data

Data on *Ae. aegypti* pupal abundance were generated from field surveys conducted in the cities of Córdoba, Orizaba, Rio Blanco, Ciudad Mendoza, Acultzingo, Maltrata, Puebla City and Atlixco from 11 July to 20 August 2011 and from the cities of Coatepec, Xalapa and Perote between 23 August and 1 September of the same year. Approximately 50 study premises were examined for each one of the 12 communities; these premises were contained within 3–4 spatially distinct clusters within each community. The methodologies for the selection of premises to examine, the collection of immature mosquitoes (larvae and pupae) from indoor and outdoor water-holding containers on the premises, the subsequent rearing to adults and species identification and, finally, the estimation of pupal abundance

for *Ae. aegypti* in the study sites were described previously by Lozano-Fuentes [30]. About 73% of collected pupae were successfully reared to adults and identified to species, compared to just 16% for collected larvae. Consequently, we focus only on the more robust estimates for pupal abundance.

Figure 1. The study area with the locations of communities in Central Mexico in relation to elevation, as estimated by the digital elevation model (DEM) of the Shuttle Radar Topographic Mission (SRTM).



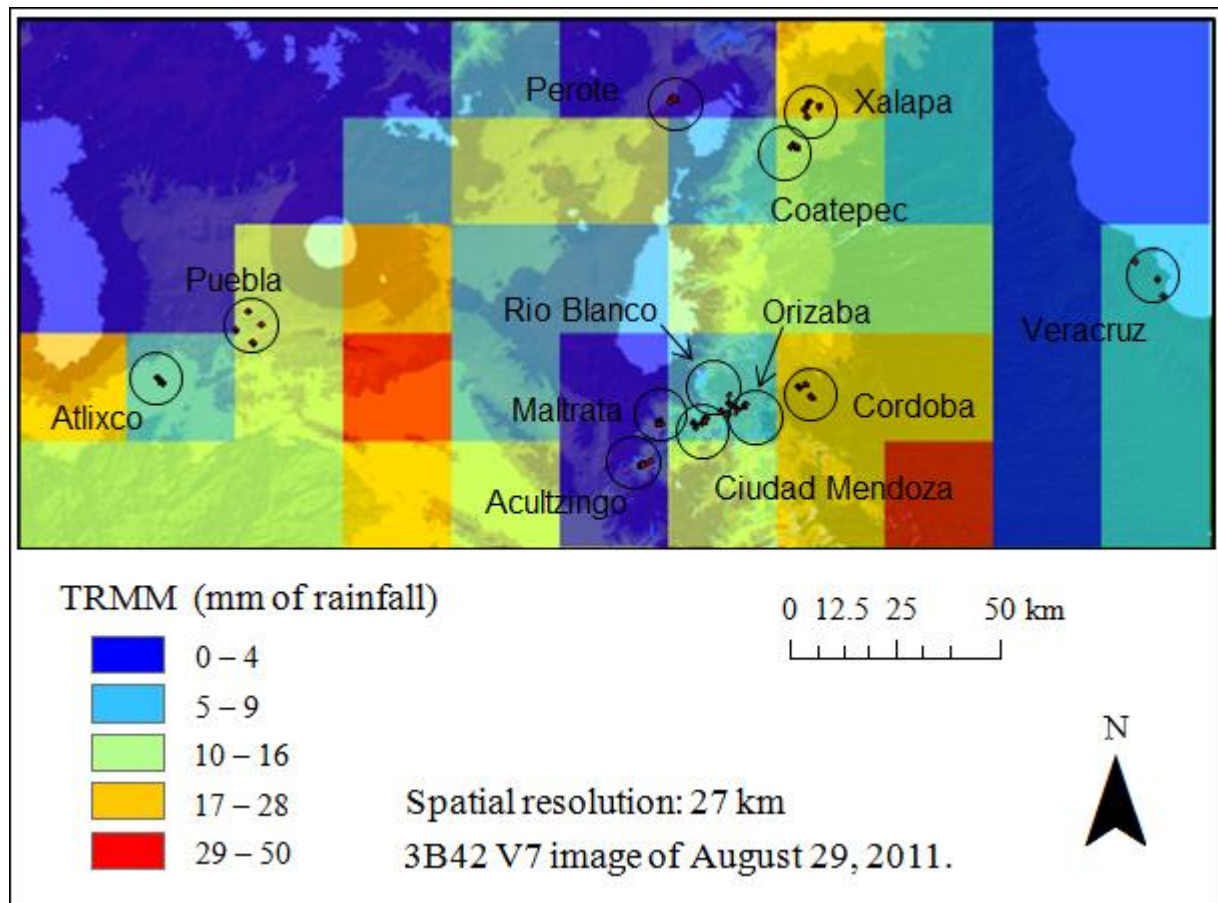
2.3. Remotely Sensed Data

2.3.1. Visible Infrared Scanner (VIRS)

Data on precipitation were estimated with product 3B42 V7 derived from the Visible Infrared Scanner (VIRS) sensor onboard the TRMM satellite and retrieved from the TRMM Online Visualization and Analysis System (TOVAS) [31]. This system is maintained by the NASA Goddard Earth Science Data and Information Services Center. The 3B42 V7 data cover the tropical and subtropical regions between 50°N and 50°S with a daily temporal resolution adjusted from a 3-hourly temporal resolution and a spatial resolution of 0.25° by 0.25°, roughly equivalent to 27 km in the study area (Figure 2). TRMM is a joint mission between the U.S. National Aeronautics and Space

Administration (NASA) and the Japan Aerospace Exploration Agency (JAXA), launched on 27 November of 1997 and designed to measure rainfall for weather and climate research. Data were processed using ArcMap 10.2 software. TRMM has been shown to reasonably reproduce rainfall variability at monthly timescales that are analogous to the four-week timescales used in this study [32].

Figure 2. Tropical Rainfall Measuring Mission (TRMM), 3B42 V7 image of 29 August 2011.



2.3.2. Moderate Resolution Imaging Spectroradiometer (MODIS)

MODIS data were downloaded from the Reverb/Echo NASA EOS Data and Information System (EOSDIS) website [33] and were processed using the MODIS Reprojection Tool (MRT) and ArcMap 10.2 software. Onboard the Terra and Aqua satellites, MODIS has been one of the most used instruments for the Earth Observing System (EOS), a NASA international program, which, in turn, is a key component of NASA's Earth Science Enterprise [34]. Launched on 18 December 1999 (Terra), and 4 May 2002 (Aqua), Terra and Aqua are designed to monitor many conditions of the atmosphere, land, oceans, biosphere and cryosphere, although their foci are on land and ocean observations, respectively [35]. Both satellites have sun-synchronous orbits crossing the equator at an approximate local time of 10:30 AM and 10:30 PM in the case of Terra and at 1:30 PM and 1:30 AM for Aqua, in a northward and southward track, respectively.

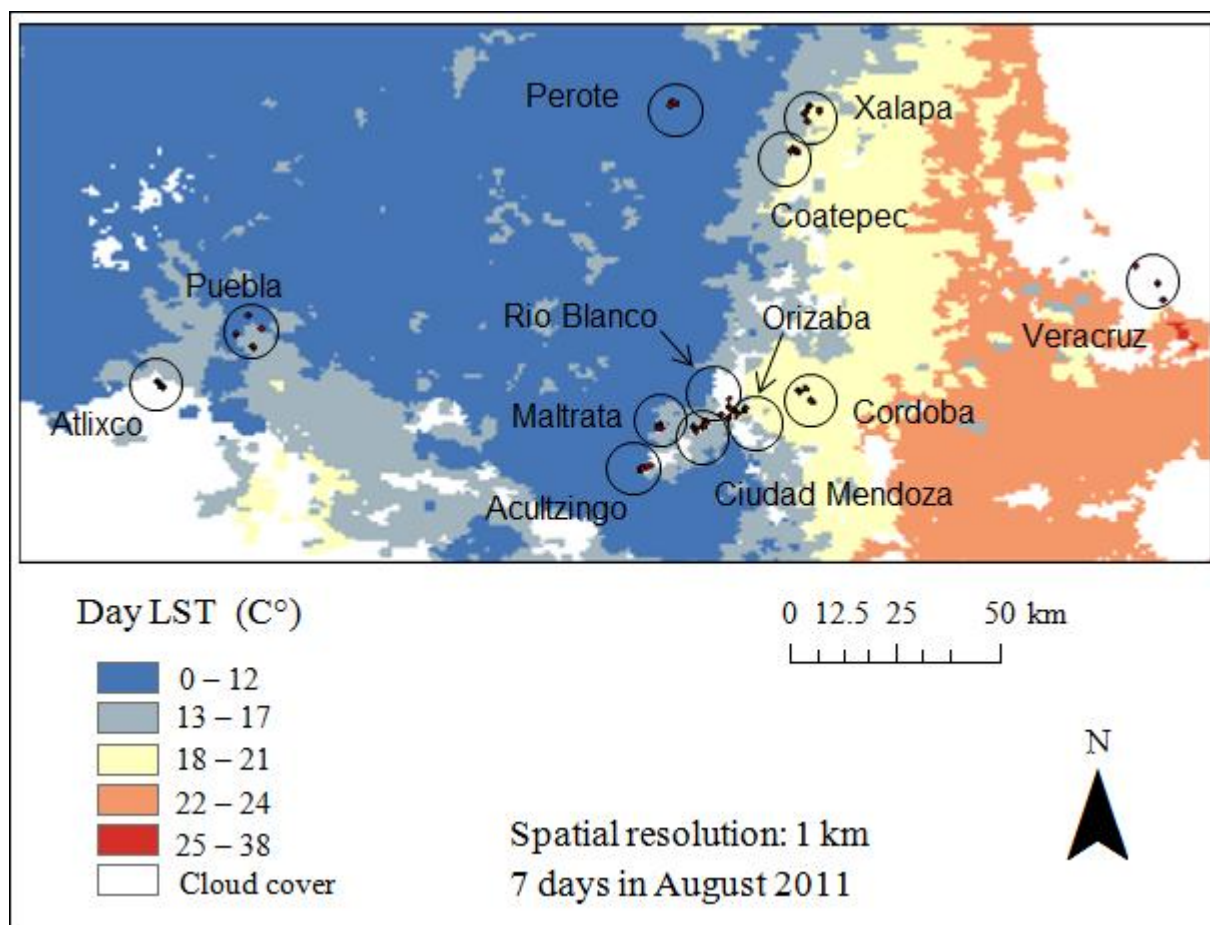
LST estimates are from the MODIS Land Surface Temperature and Emissivity product (MYD11A1) from the Aqua satellite. This product provides temperature and emissivity values per-pixel. MYD11A1 measurements along with all data generated from sensors carried by Aqua can be

obtained for the entire globe within two days [35]. The daily MYD11A1 product has a spatial resolution of 1 km (Figure 3). Previous studies have shown that MODIS LST products have generally been accurate within ± 1 K compared to *in situ* temperature measurements, for a variety of sites and conditions [36,37].

2.3.3. Shuttle Radar Topography Mission (SRTM)

Expected to be strongly associated with ambient temperature, elevation was examined as a potential proxy for temperature. Elevation was estimated through the Digital Elevation Model (DEM) from the SRTM, a collaboration between NASA and the National Imagery and Mapping Agency (NIMA) of the U.S. Department of Defense [38]. With a resolution of 90 m at the equator (Figure 1), the SRTM was designed to produce a DEM of the Earth’s land surface approximately between latitudes 60° N and 56° S. In an 11-day flight around the world onboard the Space Shuttle Endeavour, the mission was completed on 22 February 2000. The data for this study were downloaded from the Global Data Explorer website [39], which is maintained by the United States Geological Survey (USGS) and NASA’s Land Processes Distributed Active Archive Center (LPDAAC).

Figure 3. Composite of 7 days of day LST images (MYD11A1) from August 2011.



2.4. Match-Up Data Procedure

Field survey-based estimates for *Ae. aegypti* pupal abundance from the 607 examined premises were aggregated at the community and cluster levels through two approaches by estimating: (1) the percentages of premises with the presence of *Ae. Aegypti* pupae; and (2) the mean abundances of *Ae. aegypti* pupae per premises. Both types of estimates for pupal abundance were matched up with RS data derived from the location of the corresponding premises and, similarly, aggregated at the community and cluster level. RS data provided daily data for LST (nighttime and daytime), rainfall and elevation. The matched values of RS data were calculated as follows: Nighttime LST was calculated from the average nighttime cloud-free LST data for the 29 nights preceding the survey. The same process was repeated for daytime LST data, except that the average was calculated over the 28 days preceding the day of the survey plus the day of the survey. After removing cloudy days, the average number of days with daily data used to obtain the average LST values was 7.9 for nighttime LST and 6.8 for daytime LST. RS estimates of rainfall were calculated using the accumulated amount over the period comprising the day of the survey plus the 28 preceding days. No special calculation was required for elevation data, since these are a snapshot of the DEM data of the 2000 flight. Each set of matched pairs between pupae abundance and LST (day and night), rainfall and elevation were analyzed for correlation at both levels of aggregation: community and cluster, using the SAS 9.3 proc corr method.

We also tested using a two-week period instead of a four-week period preceding the field mosquito surveys, and in all cases, the correlations between climatic data and mosquito presence/abundance were lower (data not shown). A period longer than four weeks was not analyzed, since no improvement was noticed by Lozano-Fuentes *et al.* [30] when analyzing for similar correlations, but using *in situ* temperature data from HOBO meteorological stations (Onset Computer Corporation, Bourne, MA, USA) and rainfall from the Climate Prediction Center Morphing Technique (CMORPH) dataset.

3. Results

Table 1 summarizes the aggregated values per community for: (1) the percentage of premises with the presence of *Ae. aegypti* pupae; and (2) mean abundances of pupae per premises, along with the corresponding aggregated RS values for the climate variables LST (nighttime and daytime), rainfall and elevation. The table is ordered by decreasing estimated mean abundance of *Ae. Aegypti* pupae per premises. In total, a mean number of 3.8 *Ae. Aegypti* pupae were found per examined premises. The overall percentage of premises with the presence of *Ae. aegypti* pupae was 19.44%. Perote, the community at the highest elevation (2400 m) out of the 12 study communities, was the only one where no *Ae. aegypti* were found. As reported by Lozano [30] using the same data set, this was also the case when including larvae. In general, a lower percentage of presence and mean abundance values for *Ae. aegypti* occurs at the cooler, drier sites at higher elevations.

Table 1. Estimates for the abundance of *Aedes aegypti*, by study community, in relation to climate variables and elevation.

Community	Percentage	Mean	Night LST (C °)	Day LST (C °)	Rainfall (mm)	Elevation (m)
Orizaba	35	14.29	16.0	33.2	354	1236
Rio Blanco	41	10.43	15.0	30.9	334	1258
Cordoba	24	6.04	16.7	33.1	507	860
Veracruz	28	4.91	21.7	40.7	372	18
Coatepec	25	3.26	16.1	32.2	208	1203
Ciud. Mendoza	21	2.63	14.6	31.9	348	1338
Acultzingo	14	1.68	12.8	28.9	217	1695
Xalapa	24	0.98	15.4	31.8	209	1419
Atlixco	12	0.28	15.0	36.6	124	1831
Maltrata	4	0.06	10.9	29.9	210	1714
Puebla	4	0.04	11.4	35.2	112	2141
Perote	0	0.00	8.1	28.5	203	2417

Percentage: the percentage of premises with the presence of *Ae. aegypti* pupae; mean: the mean abundance of *Ae. aegypti* pupae per premise; night LST: the MODIS estimated LST (MYD11A1, night); day LST: the MODIS estimated LST (MYD11A1, day); rainfall: the TRMM estimated precipitation (3B42 V7); elevation: the SRTM's DEM estimated elevation.

3.1. Correlations among RS Estimated Climate Variables

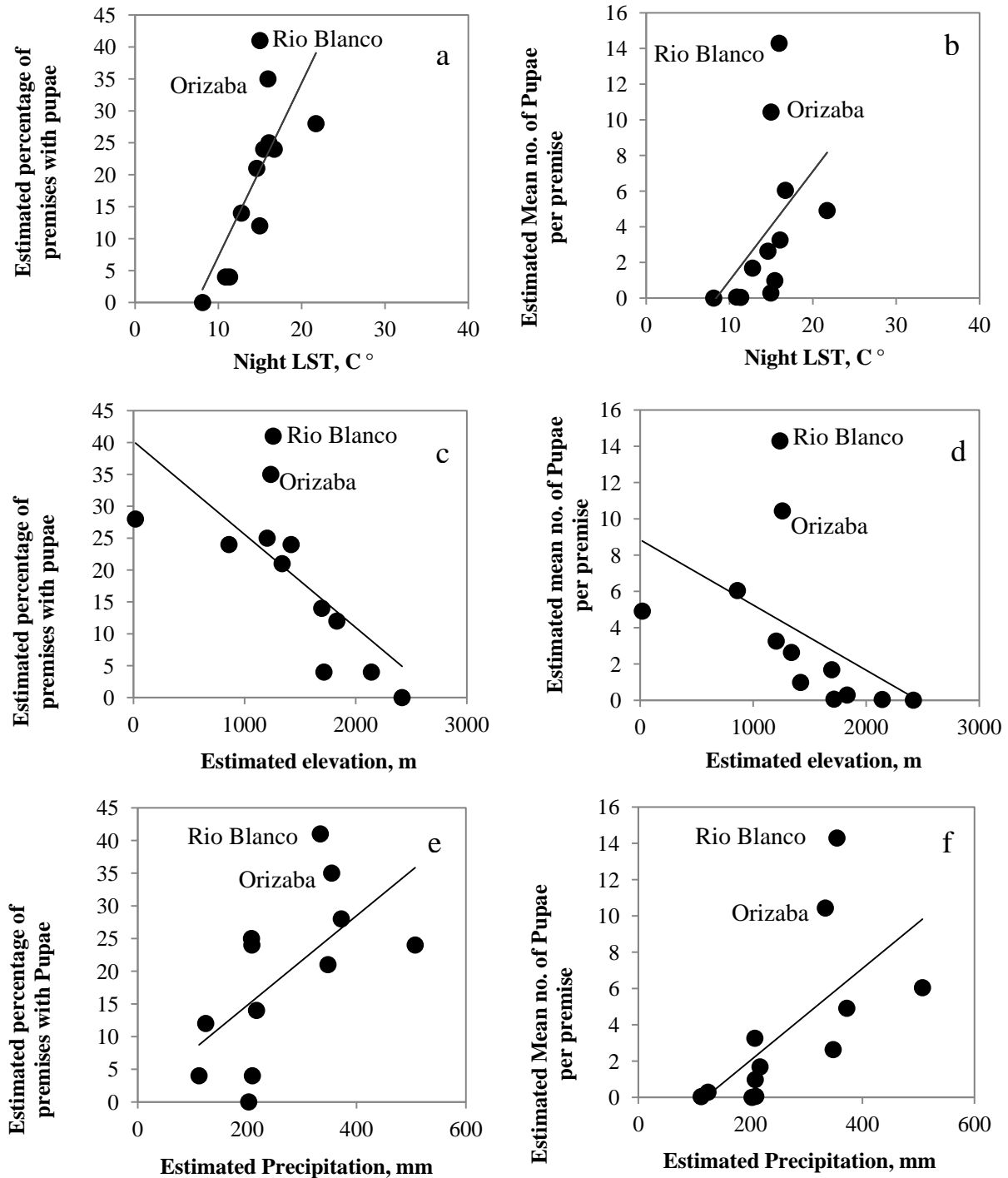
A summary of the correlation analysis of RS estimated variables with each other is presented in Table 2. An obviously expected significant correlation between the estimated values of elevation and LST was detected when using nighttime LST data, both at the community and cluster levels. However, this relationship was not significant at either level of aggregation when using daytime LST data. Elevation was significantly and inversely correlated with estimated precipitation at both levels of aggregation, community and cluster. Furthermore, as expected, there was a significant positive correlation between the LST estimates for night and day at both scale levels. Finally, for either level of aggregation, significant associations between estimated precipitation and LST were only detected with nighttime LST, but not with daytime LST.

Table 2. Summary of the Spearman correlations among the RS estimated climate variables.

Climate Variables	Community	Cluster
	N = 12	N = 43
Elevation and night LST	−0.91 **	−0.87 **
Elevation and day LST	−0.39	−0.29
Elevation and rainfall	−0.80 **	−0.80 **
Night LST and day LST	0.59 *	0.55 **
Rainfall and night LST	0.60 *	0.60 *
Rainfall and day LST	0.11	−0.008

** $p < 0.01$, * $p < 0.05$.

Figure 4. Plots at the community level. Relationships between: (a) night LST and the estimated percentage of premises (“sites”) with *Aedes aegypti* pupae present; (b) night LST and the estimated mean number of pupae per site; (c) elevation and the estimated percentage of premises with pupae present; (d) elevation and the estimated mean number of pupae per site; (e) the estimated precipitation and estimated percentage of premises with pupae present; (f) the estimated precipitation and estimated mean number of pupae per premises.



3.2. Correlations among RS-Estimated Climate Variables and Mosquito Presence and Abundance

At the community and cluster levels, Table 3 summarizes the correlation results between RS estimated climate variables and both measures of *Ae. aegypti* populations: the percentage of premises with the presence of *Ae. aegypti* pupae and mean abundances of *Ae. aegypti* pupae per premises. MODIS-estimated nighttime LST was positively and significantly correlated with the percentage of homes with *Ae. aegypti* pupae or the mean abundance of *Ae. aegypti* pupae per premises at the community (Figure 4a,b) and cluster level (plot not shown). Similarly, elevation estimated through SRTM showed a significant, although inverse, correlation with the percentage of premises with the presence of *Ae. aegypti* pupae or a mean abundance of *Ae. aegypti* pupae per premises at both levels of aggregation, community (Figure 4c,d) and cluster (plot not shown). Positive and significant correlations were detected between TRMM-estimated precipitation and the percentage of premises with the presence of *Ae. aegypti* pupae or mean abundances of *Ae. aegypti* pupae per premises at the community (Figure 4e,f) and cluster level (plot not shown). No correlation was detected between MODIS-estimated daytime LST and the percentage of premises with the presence of *Ae. aegypti* pupae or mean abundances of *Ae. aegypti* pupae per premises at any level of aggregation (plots not shown).

Table 3. Summary of Spearman correlations between RS estimated climate variables and the abundance of *Aedes aegypti* pupae.

Climate Variables	Community N = 12	Cluster N = 43
Night LST and percentage	0.82 **	0.56 **
Night LST and mean	0.78 **	0.64 **
Elevation and percentage	−0.84 **	−0.67 **
Elevation and mean	−0.87 **	−0.75 **
Rainfall and percentage	0.61 *	0.50 **
Rainfall and mean	0.79 **	0.55 **
Day LST and percentage	0.33	0.12
Day LST and mean	0.29	0.21

** $p < 0.01$, * $p < 0.05$.

4. Discussion

Associations between extreme weather events and mosquito outbreaks [40,41], as well as the weather-mediated seasonal dynamics of mosquito abundance [42] have been reported in the literature for *Ae. aegypti*. Although seasonal weather fluctuations can in large part explain intra-annual fluctuations in the abundance of *Ae. aegypti*, studies conducted at the local scale and, therefore, under very similar weather conditions, have revealed differences in vector abundance among nearby urban locations [42–44]. This likely reflects the effect of anthropogenic modifications in the urban environments that this mosquito prefers to inhabit [42,44]. Using a study design that takes advantage of a geographic transect with similar socio-economic conditions in the specific field survey areas, a previous cross-sectional analysis using this dataset for the abundance of *Ae. aegypti* and *in situ* weather data also reported significant associations between mosquito abundance and weather variables (temperature or rainfall) and elevation [30]. The uniformity in socio-economic conditions in the

specific study areas allows the opportunity to minimize the influence of the anthropogenic sources of variability, while at the same time studying elevation and weather variables at approximately the same point in time. The present study further capitalizes on such advantages by specifically focusing on testing the applicability of widely-used RS products to explore weather linkages with *Ae. aegypti* abundance at the local scale.

Despite the relatively coarse spatial resolution of 1 km for nighttime LST and approximately 26 km for rainfall, strong correlations were found between data from the MYD11A1 product or 3B42 V7, respectively, and the local abundance of *Ae. aegypti* pupae. Conversely, the results were not encouraging for daytime LST. Honório *et al.* [45] showed a positive linear relationship between mosquito abundance and ambient temperature within a range of 18 °C to 24 °C. The authors did not detect any variation in the abundance of *Ae. aegypti* above this temperature threshold. Further, Eisen *et al.* [46] reported a positive linear relationship between water temperature and the development rate for immature *Ae. aegypti* between 15 °C to 30 °C. In that study, lower developmental zero temperatures were estimated to be in the 10 °C to 14 °C range for eggs and immature *Ae. aegypti* and the upper developmental zero temperatures in the 38 °C to 42 °C range. It is interesting to notice that in our study, the mean cluster level daytime LST ranged from 27.5 °C to 40.7 °C while the nighttime LST ranged from 7.8 °C to 24.2 °C, which included the range of positive correlation reported by Honório *et al.* [45] and partially overlapped with that reported by Eisen *et al.* [46]. Additional work is needed to assess the correlations between the abundance of *Ae. aegypti* and RS data for a broader range of temperatures than examined in the present study, especially for the higher end temperatures. Similar to our results with RS data, positive linear relationships with nighttime LST, but not with daytime LST, were detected in malaria prediction models [47].

As expected from the strong positive correlation between the abundance of *Ae. aegypti* and night LST, there was also a strong, but negative, correlation between mosquito abundance and elevation. In general, a negative relationship is expected between elevation and temperature [48]; in our case, however, this was detected only when considering night LST, but not when considering day LST. Indeed, daytime LST was only associated with nighttime LST and not associated with any other variable, including elevation. This may be related to more cloud cover during the daytime than at nighttime, as suggested by the lower mean number of cloud-free images available in the daytime LST data (6.8 images, Figure 3) compared to 7.9 images available for nighttime LST data. The effect of minimum temperatures may be another contributing factor; Lozano-Fuentes *et al.* [30] identified the mean minimum daily temperature and the mean minimum daily winter temperature among the weather parameters with potential relevance for the biology of *Ae. aegypti*. Although our study did not consider these specific parameters, it is possible that minimum temperatures (which occur in our night LST data) in general may play an important role in the biology of *Ae. aegypti*.

Finally, a strong correlation has been reported between median family income and surface temperature during the daytime, with a much weaker correlation at nighttime [49]. The specific areas (*i.e.*, neighborhoods within communities) used in this study were selected under the criteria of being urban low- to middle-income homes with small- to medium-sized yards. The study premises often harbored considerable vegetation, and it is known that leaf temperatures and other vegetative features are a major aspect related to urban temperature [50]. Although, the possibility exists that income factors play a role in the differences detected between daytime and nighttime LST, such a possibility is

not evident in our study, since many of our communities were small and not likely to influence the urban heat island effect as detected in a 1-km \times 1-km grid box.

While it is possible to explain the positive correlation between RS estimated rainfall and the abundance of *Ae. aegypti* in terms of more containers being filled with rain water (or some containers having a greater volume of water) and, thus, more potential larval development sites when it rains, this could be a casual association, due to the fact that the areas with higher temperature and lower elevation also typically have a higher rainfall. Indeed, rainfall and nighttime LST were weakly, but significantly and positively correlated. It also should be noted that the impact of rainfall on the presence of larval development sites for *Ae. aegypti* is complicated by human water storage practices, with the importance of containers filled by rain *versus* human action varying both among geographic areas and within the year in single locations. However, the results found in this study are consistent with those of Lozano-Fuentes *et al.* [30] using meteorological data from weather stations along the same transect. Additionally, our results are consistent with process-based life-cycle models of *Ae. aegypti*; mosquito populations become largest when temperatures are warm and rainfall is abundant [51,52]. They are also consistent with studies indicating that dengue risk in humans is positively correlated with temperature and rainfall [53], which is likely in part due to the impacts of temperature and rainfall on vector populations [54,55].

The apparent outlier of Rio Blanco and Orizaba depicted in Figure 4 is also clear in table of Lozano-Fuentes *et al.* [30], when using data on both pupae and larvae. We found that in general, the relationship between *Ae. aegypti* pupal abundance and temperature/rainfall is robust in the higher elevation regions (above \sim 1300 m ASL) and is weaker at lower elevations (below \sim 1300 m ASL). We believe the weaker relationship between temperature/rainfall and pupal abundance below \sim 1300 m in our study region is an indicator that once temperature and rainfall increase to a certain point, pupae are abundant no matter how much warmer or wetter it becomes; *i.e.*, the climate is ideal for immature *Ae. aegypti* development anywhere in the warm, wet regions below \sim 1300 m. From a mathematical standpoint, this observation indicates that the relationship between pupal abundance and climate variability likely becomes more asymptotic below \sim 1300 m, so the linear fits shown in Figure 4 may oversimplify what is in reality a non-linear relationship. However, for the purposes of our paper, in which we are simply trying to show that LST, rainfall and elevation are correlated with *Ae. aegypti* pupal abundance, these linear fits are adequate. It may also be possible that the comparatively greater urban density of Orizaba and Rio Blanco (Rio Blanco is a dormitory city of Orizaba) may be more favorable for higher numbers of *Ae. aegypti*, perhaps because of the sheer numbers of container habitats. In support of this conjecture, Coatepec has similar characteristics of elevation and temperature (although slightly lower rainfall) compared to Orizaba and Rio Blanco, but lower urban density; and it has also a lower presence and abundance of *Ae. aegypti* pupae (Table 1).

The findings of this study suggest the promise for future RS-based predictive models of *Ae. aegypti* population fluctuations and other applications, such as dengue outbreak prediction [56]. These results are even more promising when considering future remote sensing products with enhanced capabilities that may be available soon via new or planned NASA and/or partner missions. Of special note are the Visible Infrared Imaging Radiometer Suite (NPP-VIIRS), the Global Precipitation Measurement (GPM) mission and the Soil Moisture Active Passive (SMAP) mission. Carried onboard the Suomi National Polar-orbiting Partnership (NPP) satellite, the VIIRS sensor will use visible and infrared

wavelengths to study land, atmosphere, ice and ocean. Besides LST, VIIRS will make observations on active fires, vegetation, ocean color, sea surface temperature and other surface features available to the scientific community [57]. These observations will facilitate the study of climate change, clouds and aerosols; phytoplankton and sediment in the seas; forest cover and productivity; and changes in polar sea ice. The similarities between VIIRS and MODIS will provide continuity for monitoring programs conducted with MODIS. The Global Precipitation Measurement (GPM) mission will provide continuity to TRMM data to monitor precipitation and for other hydrological applications [58]. Measuring soil moisture present at the Earth's land surface, the Soil Moisture Active Passive (SMAP) mission will be critical to flood assessment and drought monitoring, as well as to the study of the global carbon balance [59]. SMAP is expected to be another undertaking that will play an important role in the monitoring of environmental variables associated not just with vector transmitted diseases in general, but also, and especially, soil transmitted helminthes infections. Soil moisture is a critical determinant for the survival of helminth eggs in the soil [60–62].

The application of the remotely-sensed products in this study was useful for identifying correlations between environmental variables and the presence and abundance of *Ae. aegypti*. This finding is encouraging for using these products to identify areas most at risk of high pupal abundance at local scales on the order of 1-km. It is tempting to speculate that if these products work at the local scale for cities along our topographically complex transect in Mexico, they would work even better in areas where the topographic variability is comparatively smaller (and therefore, environmental variables do not vary as much in space), for example, in the southern part of the continental United States. However, since the abundance of *Ae. aegypti* is also closely linked to the characteristics of the human environment, it is imperative to also consider the potential confounding effects of socioeconomic and human ecology (e.g., housing style, water storage, *etc.*) factors associated with mosquito establishment and proliferation [3,63]. In addition to affecting mosquito abundance, socio-economic factors can play a role in the vulnerability of human inhabitants to dengue virus infection; for example, Hagenlocher *et al.* [63] constructed a composite index of socioeconomic vulnerability to dengue that included both indicators of susceptibility, as well as a lack of resilience.

An overarching goal, whether focusing on mosquito vector abundance, vector infection rates and the risk of virus transmission to humans, socioeconomic vulnerability or the risk for dengue epidemics, is to give public health professionals and the general public time to prepare for and attempt to prevent or mitigate disease outbreaks. For example, researchers have determined that the optimal lead time for dengue early warning for officials in Singapore would be three months in order to suppress an epidemic [64], and global risk maps have been developed to estimate the risk of dengue in Europe [65]. Better defining the linkages between environmental and climatic conditions and the incidence and geographic spread of mosquito vectors and dengue, together with the ability to use remotely-sensed observations to detect conditions signaling increased risk, would be of great value for future outbreak prediction and disease suppression.

5. Conclusions

Strong correlations were found between the abundance of the dengue virus mosquito vector, *Ae. aegypti*, and RS-derived nighttime LST, elevation or rainfall along a geographic climate/elevation

gradient in Central Mexico. The results were consistent with what was found by Lozano-Fuentes *et al.* [30] using data from the same mosquito field surveys, but meteorological data from weather stations. These findings show that data from the three analyzed RS products can be used to predict *Ae. Aegypti* abundance, but further studies are needed to define the climatic and socio-economic conditions under which the correlations observed herein can be assumed to apply.

Acknowledgments

This study was funded by grants from the National Aeronautic and Space Administration (NASA) and the National Science Foundation (NSF). The NASA funds were granted through ROSES-2010: Earth Science Applications Feasibility Studies: Public Health (A.31); and to the Applied Earth Sciences group at the Marshall Space Flight Center (MSFC) (10-PHFEAS10-0010). The NSF funds were granted to the University Corporation for Atmospheric Research (GEO-1010204). The National Center for Atmospheric Research is partially funded by NSF. A partial contribution was provided by an appointment to the NASA Postdoctoral Program at the Marshall Space Flight Center/National Space Science and Technology Center/NASA Global Hydrology and Climate Center in Huntsville, AL, USA; administered by Oak Ridge Associated Universities through a contract with NASA. We express our appreciation to Douglas Rickman and Mohammad Z. Al-Hamdan for their guidance in the processing of remote sensing applications, as well as to SERVIR for providing logistics and support. We thank Gina Wade for helping with the proposal. We also thank Carolina Ochoa-Martinez and Berenice Tapia-Santos for running the field teams and to Kevin Kobylinski and Chris Uejio for helping out in the field. Lastly but not the least we thank the students from Veracruz University who helped with the field work completing the survey and collecting the *in situ* data.

Author Contributions

Max J. Moreno-Madriñán is the main author who conceived and designed the manuscript, processed most of the remote sensing applications, performed the analyses, wrote most of the manuscript and participated in a portion of the field *in situ* data collection. Lars Eisen, and Andrew J. Monaghan contributed in the writing of the manuscript and analysis of results. William L. Crosson revised the manuscript and along with the first author and Andrew J. Monaghan, Saul Lozano-Fuentes, Sue M. Estes, Maurice G. Estes, Mary Hayden and Emily Zielinski-Gutierrez participated in the field collecting *in situ* data. Sarah N. Hemmings contributed in the writing of the manuscript. Mary Hayden, Lars Eisen and Saul Lozano-Fuentes conceived the initial study while Sue Estes, William L. Crosson, Maurice G. Estes and Dale Quattrochi conceived the extension to remote sensing applications. Carlos M. Welsh-Rodriguez coordinated the survey for *in situ* data collection and facilitated the logistics needed. Saul Lozano-Fuentes wrote the field protocol, trained the field teams, and led most of the field work. William L. Crosson, Maurice G. Estes, Dan E. Irwin and Dale Quattrochi contributed in the processing of remote sensing applications. Dan E. Irwin facilitated the logistics required for the remote sensing work, the connection with end-users and the means for this study to happen. All authors read and approved the final manuscript.

Conflicts of Interest

The authors declare no conflict of interest.

References

1. Epstein, P.R. Climate change and emerging infectious disease. *Microbes Infect.* **2001**, *3*, 747–754.
2. Githeko, A.K.; Lindsay, S.W.; Confalonieri, U.E.; Patz, J.A. Climate change and vector-borne diseases: A regional analysis. *Bull. World Health Organ.* **2000**, *78*, 1136–1147.
3. Gubler, D.J.; Reiter, P.; Ebi, K.L.; Yap, W.; Nasci, R.; Patz, J.A. Climate variability and change in the United States: Potential impacts on vector and rodent-borne diseases. *Environ. Health Perspect.* **2001**, *109* (Suppl. S2), 223–233.
4. Haines, A.; Kovats, R.S.; Campbell-Lendrum, D.; Corvalan, C. Climate change and human health: Impacts, vulnerability and public health. *Public Health* **2006**, *120*, 585–596.
5. Lafferty, K.D. The ecology of climate change and infectious diseases. *Ecol. Soc. Am.* **2009**, *90*, 888–900.
6. McMichael, A.J.; Woodruff, R.E.; Hales, S. Climate change and human health: Present and future risk. *Lancet* **2006**, *367*, 859–869.
7. Ceccato, P.; Connor, S.J.; Jeanne, I.; Thomson, M.C. Application of geographical information systems and remote sensing technologies for assessing and monitoring malaria risk. *Parassitologia* **2005**, *47*, 81–96.
8. Mills, J.N.; Gage, K.L.; Khan, A.S. Potential influence of climate change on vector-borne and zoonotic diseases: A review and proposed research plan. *Environ. Health Perspect.* **2010**, *118*, 1507–1514.
9. Parkinson, A.J.; Butler, J.C. Potential impacts of climate change on infectious diseases in the Arctic. *Int. J. Circumpolar Health* **2005**, *64*, 478–486.
10. Semenza, J.C.; Menne, B. Climate change and infectious diseases in Europe. *Lancet Infect. Dis.* **2009**, *9*, 365–375.
11. Allen, T.R.; Wong, D.W. Exploring GIS, spatial statistics and remote sensing for risk assessment of vector-borne diseases: A West Nile virus example. *Int. J. Risk Asmt. Mgmt.* **2006**, *6*, 253–275.
12. Hay, S.I.; Packer, M.J.; Rogers, D.J. The impact of remote sensing on the study and control of invertebrate intermediate hosts and vectors for disease. *Int. J. Remote Sens.* **1997**, *18*, 2899–2930.
13. Hay, S.I.; Snow, R.W.; Rogers, D.J. From predicting mosquito habitat to malaria seasons using remotely sensed data: Practice, problems and perspectives. *Parasitol. Today* **1998**, *14*, 306–313.
14. Kalluri, S.; Gilruth, P.; Rogers, D.; Szczur, M. Surveillance of arthropod vector-borne infectious disease using remote sensing techniques: A review. *PLoS Pathog.* **2007**, *3*, 1361–1371.
15. Gubler, D.J.; Clark, G.G. Dengue/Dengue hemorrhagic fever: The emergence of a global health problem. *Emerg. Infect. Dis.* **1995**, *1*, 55–57.
16. Bhatt, S.; Gething, P.W.; Brady, O.J.; Messina, J.P.; Farlow, A.W.; Moves, C.L.; Drake, J.M.; Brownstein, J.S.; Hoen, A.G.; Sankoh, O.; *et al.* The global distribution and burden of dengue. *Nature* **2013**, *496*, 504–507.

17. Brunkard, J.M.; Robles Lopez, J.L.; Ramirez, J.; Cifuentes, E.; Rothenberg, S.J.; Hunsperger, E.A.; Moore, C.G.; Brussolo, R.M.; Villarreal, N.A.; Haddad, B.M. Dengue fever seroprevalence and risk factors, Texas-Mexico border, 2004. *Emerg. Infect. Dis.* **2007**, *13*, 1477–1483.
18. Chowell, G.; Sanchez, F. Climate-based descriptive models of dengue fever: The 2002 epidemic in Colima, Mexico. *J. Environ. Health* **2006**, *68*, 40–44.
19. Chowell, G.; Cazelles, B.; Broutin, H.; Munayco, C.V. The influence of geographic and climate factors on the timing of dengue epidemics in Peru, 1994–2008. *BMC Infect. Dis.* **2011**, *11*, doi:10.1186/1471-2334-11-164.
20. Colon-Gonzalez, F.J.; Lake, I.R.; Bentham, G. Climate variability and dengue fever in warm and humid Mexico. *Am. J. Trop. Med. Hyg.* **2011**, *84*, 757–763.
21. Degallier, N.; Favier, C.; Menkes, C.; Lengaigne, M.; Ramalho, W.M.; Souza, R.; Servain, J.; Boulanger, J.P. Toward an early warning system for dengue prevention: Modeling climate impact on dengue transmission. *Clim. Chang.* **2010**, *98*, 581–592.
22. Fuller, D.O.; Troyo, A.; Beier, J.C. El Nino Southern Oscillation and vegetation dynamics as predictors of dengue fever cases in Costa Rica. *Environ. Res. Lett.* **2009**, *4*, 140111–140118.
23. Herrera-Martinez, A.D.; Rodriguez-Morales, A.J. Potential influence of climate variability on dengue incidence registered in a western pediatric hospital of Venezuela. *Trop. Biomed.* **2010**, *27*, 280–286.
24. Hurtado-Diaz, M.; Riojas-Rodriguez, H.; Rothenberg, S.J.; Gomez-Dantes, H.; Cifuentes, E. Short communication: Impact of climate variability on the incidence of dengue in Mexico. *Trop. Med. Int. Health* **2007**, *12*, 1327–1337.
25. Johansson, M.A.; Cummings, D.A.T.; Glass, G.E. Multiyear climate variability and dengue-El Nino Southern Oscillation, weather, and dengue incidence in Puerto Rico, Mexico, and Thailand: A longitudinal data analysis. *PLoS Med.* **2009**, *6*, doi:10.1371/journal.pmed.1000168.
26. Johansson, M.A.; Dominici, F.; Glass, G.E. Local and global effects of climate on dengue transmission in Puerto Rico. *PLoS Negl. Trop. Dis.* **2009**, *3*, doi:10.1371/journal.pntd.0000382.
27. Lowe, R.; Bailey, T.C.; Stephenson, D.B.; Graham, R.J.; Coelho, C.A.S.; Carvalho, M.S.; Barcellos, C. Spatiotemporal modelling of climate-sensitive disease risk: Towards an early warning system for dengue in Brazil. *Comput. Geosci.* **2011**, *37*, 371–381.
28. Machado-Machado, E.A. Empirical mapping of suitability to dengue fever in Mexico using species distribution modeling. *Appl. Geogr.* **2012**, *33*, 82–93.
29. Eisen, L.; Moore, C.G. *Aedes (Stegomyia) aegypti* in the Continental United States: A vector at the cool margin of its geographic range. *J. Med. Entomol.* **2013**, *50*, 467–478.
30. Lozano-Fuentes, S.; Hayden, M.H.; Welsh-Rodriguez, C.; Ochoa-Martinez, C.; Tapia-Santos, B.; Kobylinski, K.C.; Uejio, C.K.; Zielinski-Gutierrez, E.; Monache, L.D.; Monaghan, A.J.; *et al.* The dengue virus mosquito vector *Aedes aegypti* at high elevation in México. *Am. J. Trop. Med. Hyg.* **2012**, *87*, 902–909.
31. Online Visualization and Analysis System (TOVAS). Available online: <http://disc.sci.gsfc.nasa.gov/precipitation/tovas> (accessed on 6 September 2013).
32. Huffman, G.J.; Coauthors. The TRMM multisatellite Precipitation Analysis (TMPA): Quasi-global, multiyear, combined-sensor precipitation estimates at fine scales. *J. Hydrometeorol.* **2007**, *8*, 38–55.

33. Reverb/Echo NASA EOS Data and Information System (EOSDIS) Website. Available online: <http://reverb.echo.nasa.gov/reverb/> (accessed on 20 December 2013).
34. Xiong, X.; Barnes, W. An overview of MODIS radiometric calibration and characterization. *Adv. Atmos. Sci.* **2006**, *23*, 69–79.
35. Parkinson, C.L. Aqua: An earth-observing satellite mission to examine water and other climate variables. *IEEE Trans. Geosci. Remote Sens.* **2003**, *41*, 173–183.
36. Coll, C.; Caselles, V.; Galve, J.M.; Valor, E.; Niclòs, R.; Sánchez, J.M.; Rivas, R. Ground measurements for the validation of land surface temperatures derived from AATSR and MODIS data. *Remote Sens. Environ.* **2005**, *97*, 288–300.
37. Wan, Z.; Zhang, Y.; Zhang, Y.Q.; Li, Z-L. Validation of the land-surface temperature products retrieved from Moderate Resolution Imaging Spectroradiometer data. *Remote Sens. Environ.* **2002**, *83*, 163–180.
38. Farr, T.G.; Rosen, P.A.; Caro, E.; Crippen, R.; Duren, R.; Hensley, S.; Kobrick, M.; Paller, M.; Rodriguez, E.; Roth, L.; *et al.* The shuttle radar topography mission. *Rev. Geophys.* **2007**, *45*, doi:10.1029/2005RG000183.
39. Global Data Explorer. Available online: <http://gdex.cr.usgs.gov/gdex/> (accessed on 7 October 2013).
40. Chaves, L.F.; Morrison, A.C.; Kitron, U.D.; Scott, T.W. Nonlinear impacts of climatic variability on the density-dependent regulation of an insect vector of disease. *Glob. Chang. Biol.* **2012**, *18*, 457–468.
41. Chaves, L.F.; Scott, T.W.; Morrison, A.C.; Takada, T. Hot temperatures can force delayed mosquito outbreaks via sequential changes in *Aedes aegypti* demographic parameters in autocorrelated environments. *Acta Trop.* **2014**, *129*, 15–24.
42. Lana, R.M.; Carneiro, T.G.S.; Honório, N.A.; Codeco, C.T. Seasonal and nonseasonal dynamics of *Aedes aegypti* in Rio de Janeiro, Brazil: Fitting mathematical models to trap data. *Acta Trop.* **2014**, *129*, 25–32.
43. Marteis, L.; Makowski, L.; Conceicao, K.; La Corte, R. Identification and spatial distribution of key premises for *Aedes aegypti* in the Porto Dantas neighborhood, Aracaju, Sergipe State, Brazil. *Cad. Saude Publica* **2013**, *29*, 368–378.
44. Rubio, A.; Cardo, M.V.; Carbajo, A.E.; Vezzani, D. Imperviousness as a predictor for infestation levels of container-breeding mosquitoes in a focus of dengue and Saint Louis encephalitis in Argentina. *Acta Trop.* **2013**, *128*, 680–685.
45. Honório, N.A.; Codeco, C.T.; Alves, F.C.; Magalhães, M.A.F.M.; Lourenco-de-Oliveira, R. Temporal distribution of *Aedes aegypti* in different districts of Rio de Janeiro, Brazil, measured by two types of traps. *J. Med. Entomol.* **2009**, *46*, 1001–1014.
46. Eisen, L.; Monaghan, A.J.; Lozano-Fuentes, S.; Steinhoff, D.F.; Hayden, M.H.; Bieringer, P.E. The impact of temperature on the bionomics of *Aedes (Stegomyia) aegypti*, with special reference to the cool geographic range margins. *J. Med. Entomol.* **2014**, in press.
47. Riedel, N.; Vounatsou, P.; Miller, J.M.; Gosoni, L.; Chizema-Kawesha, E.; Mukonka, V.; Steketee, R.W. Geographical patterns and predictors of malaria risk in Zambia: Bayesian geostatistical modelling of the 2006 Zambia national malaria indicator survey (ZMIS). *Malar. J.* **2010**, *9*, 1–13.

48. Gebremariam, Y.B. Formulating the Relationship between Temperature and Elevation and Evaluating the Influence of Major Land Covers on Surface Temperature (A Case Study in Part of Northern Ethiopia). Available online: <http://www.scribd.com/doc/21553665/> (accessed on 20 March 2014).
49. Buyantuyev, A.; Wu, J. Urban heat islands and landscape heterogeneity: Linking spatiotemporal variations in surface temperatures to land-cover and socioeconomic patterns. *Landsc. Ecol.* **2010**, *25*, 17–33.
50. O'Rourke, P.A.; Terjung, W.H. Relative influence of city structure on canopy photosynthesis. *Int. J. Biomet.* **1981**, *25*, 1–19.
51. Focks, D.A.; Haile, D.G.; Daniels, E.; Mount, G.A. Dynamic life table model for *Aedes aegypti* (Diptera: Culicidae): Analysis of the literature and model development. *J. Med. Entomol.* **1993**, *30*, 1003–1017.
52. Focks, D.A.; Haile, D.G.; Daniels, E.; Mount, G.A. Dynamic life table model for *Aedes aegypti* (Diptera: Culicidae): Simulation results and validation. *J. Med. Entomol.* **1993**, *30*, 1018–1028.
53. Gomes, A.F.; Nobre, A.A.; Cruz, O.G. Temporal analysis of the relationship between dengue and meteorological variables in the city of Rio de Janeiro, Brazil, 2001–2009. *Cad. Saúde Pública* **2012**, *28*, 2189–2197.
54. Alto, B.W.; Bettinardi, D. Temperature and dengue virus infection in mosquitoes: Independent effects on the immature and adult stages. *Am. J. Trop. Med. Hyg.* **2013**, *88*, 497–505.
55. Lambrechts, L.; Paaïjmans, K.P.; Fansiri, T.; Carrington, L.B.; Kramer, L.D.; Thomas, M.B.; Scott, T.W. Impact of daily temperature fluctuations on dengue virus transmission by *Aedes aegypti*. *Proc. Natl. Acad. Sci. USA* **2011**, *108*, 7460–7465.
56. Buczak, A.L.; Koshute, P.T.; Babin, S.M.; Feighner, B.H.; Lewis, S.H. A data-driven epidemiological prediction method for dengue outbreaks using local and remote sensing data. *BMC Med. Inform. Decis. Mak.* **2012**, *12*, 1–20.
57. NPOESS Preparatory Project (NPP): Building a Bridge to a New Era of Earth Observations. Available online: http://www.nasa.gov/pdf/596329main_NPP_Brochure_ForWeb.pdf (accessed on 7 March 2014).
58. Kidd, C.; Hou, A. The Global Precipitation Measurement (GPM) Mission: Hydrological Applications. In Proceedings of the 2012 EUMETSAT Meteorological Satellite Conference, Sopot, Poland, 3–7 September 2012.
59. Entekhabi, B.D.; Njoku, E.G.; O'Neill, P.E.; Kellogg, K.H.; Crow, W.T.; Edelstein, W.N.; Entin, J.K.; Goodman, S.D.; Jackson, T.J.; Johnson, J.; *et al.* The soil moisture active passive (SMAP) mission. *Proc. IEEE* **2010**, doi:10.1109/JPROC.2010.2043918.
60. Bethony, J.; Brooker, S.; Albonico, M.; Geiger, S.M.; Loukas, A.; Diemert, D.; Hotez, P.J. Soil-transmitted helminth infections: Ascariasis, trichuriasis, and hookworm. *Lancet* **2006**, *367*, 1521–1532.
61. Brooker, S.; Michael, E. The potential of geographical information systems and remote sensing in the epidemiology and control of human helminth infections. *Adv. Parasitol.* **2000**, *47*, 245–270.

62. Moreno-Madriñán, M.J.; Parajón, D.G.; Al-Hamdan, M.Z.; Martinez, R.; Rickman, D.L.; Parajon, L.; Estes, S. Use of Remote Sensing/Geographical Information Systems (RS/GIS) to Identify Environmental Limits of Soil Transmitted Helminthes (STHs) Infection in Boaco, Nicaragua. In Proceedings of American Public Health Association (APHA) 139th Annual Meeting and Exposition. Washington DC, USA, 29 October–2 November 2011. Available online: <http://ntrs.nasa.gov/archive/nasa/casi.ntrs.nasa.gov/20120001772.pdf> (accessed on 9 May 2014).
63. Hagenlocher, M.; Delmelle, E.; Casas, I.; Kienberger, S. Assessing socioeconomic vulnerability to dengue fever in Cali, Colombia: Statistical vs. expert-based modeling. *Int. J. Health Geogr.* **2013**, *12*, doi:10.1186/1476-072X-12-36.
64. Hii, Y.L.; Rocklöv, J.; Wall, S.; Ng, L.C.; Tang, C.S.; Ng, N. Optimal lead time for dengue forecast. *PLoS Negl. Trop. Dis.* **2012**, *6*, doi:10.1371/journal.pntd.0001848.
65. Rogers, D.J.; Suk, J.E.; Semenza, J.C. Using global maps to predict the risk of dengue in Europe. *Acta Trop.* **2014**, *129*, 1–14.

© 2014 by the authors; licensee MDPI, Basel, Switzerland. This article is an open access article distributed under the terms and conditions of the Creative Commons Attribution license (<http://creativecommons.org/licenses/by/3.0/>).